

# Scaling Test-time Inference for Visual Grounding

Guanqi Zhan<sup>1,3\*</sup>, Changye Li<sup>4\*</sup>, Zhijian Liu<sup>1</sup>, Yao Lu<sup>1</sup>, Yi Wu<sup>4</sup>, Song Han<sup>1,2</sup>, Ligeng Zhu<sup>1</sup>  
<sup>1</sup>NVIDIA    <sup>2</sup>MIT    <sup>3</sup>University of Oxford    <sup>4</sup>Tsinghua University

Github: <http://github.com/NVlabs/EGM>

Website: <https://nvlabs.github.io/EGM>

## Abstract

*Visual grounding is an essential capability of Visual Language Models (VLMs) to understand the real physical world. Previous state-of-the-art grounding visual language models usually have large model sizes, making them heavy for deployment and slow for inference. However, we notice that the sizes of visual encoders are nearly the same for small and large VLMs and the major difference is the sizes of the language models. Small VLMs fall behind larger VLMs in grounding because of the difference in language understanding capability rather than visual information handling. To mitigate the gap, we introduce ‘Efficient visual Grounding language Models’ (EGM): a method to scale the test-time computation (#generated tokens). Scaling the test-time computation of a small model is deployment-friendly, and yields better end-to-end latency as the cost of each token is much cheaper compared to directly running a large model. On the RefCOCO benchmark, our **EGM-Qwen3-VL-8B** demonstrates **91.4 IoU** with an average of 737ms (**5.9× faster**) latency while **Qwen3-VL-235B** demands 4,320ms to achieve **90.5 IoU**. To validate our approach’s generality, we further set up a new amodal grounding setting that requires the model to predict both the visible and occluded parts of the objects. Experiments show our method can consistently and significantly improve the vanilla grounding and amodal grounding capabilities of small models to be on par with or outperform the larger models, thereby improving the efficiency for visual grounding.*

## 1. Introduction

Visual grounding is an essential capability of Visual Language Models (VLMs) to understand the physical world, especially if we want to deploy models to autonomous driving or robotics systems, where it is important to locate the tar-

get objects accurately according to the natural language instructions. Previous state-of-the-art visual grounding large language models, e.g., InternVL-3.5-241B-A28B [42] and Qwen3-VL-235B-A22B-Thinking [6], usually have large model sizes to achieve the best performance.

A natural question then arises here: **What makes small VLMs fall behind bigger VLMs for visual grounding?** To answer the question, we start with the analysis of what causes small models to fall behind bigger models for visual grounding as in Section 3. For example, in the Qwen [2, 6] family, the visual encoder is the same across different sized VLMs, and the major difference is that larger models are built with a bigger Large Language Model (LLM). We hypothesize that *the gap between different sized VLMs mainly comes from their text understanding ability rather than visual information handling*. We thoroughly verify it by visualizing the failure cases of a small model, e.g., InternVL3-8B. We find that a prominent failure pattern is ‘COMPLEX\_PROMPT’, where the text prompt is semantically complicated and there are multiple similar candidates in the image (Figure 2). This failure pattern is gradually resolved as the model size increases.

This analysis suggests a pathway towards overcoming the ‘COMPLEX\_PROMPT’ failure pattern, by enhancing the text understanding ability of small models and mitigating the performance gap with larger models. More specifically, as detailed in Section 4, we adopt GPT [17] to generate the detailed reasoning process of how to reach the target grounding box and use it to construct Supervised Fine-tuning (SFT) data for training. After the model learns the reasoning process, it is further trained with Reinforcement Learning (RL) to enhance the grounding capability. Furthermore, we set up a new grounding setting – amodal grounding, which requires the model to predict both the visible and occluded parts of the object, and apply our method in the new amodal grounding task.

We conduct experiments on state-of-the-art open-source visual language models including QwenVL and InternVL in Section 5. Results show our method can consistently

\*Equal contribution.

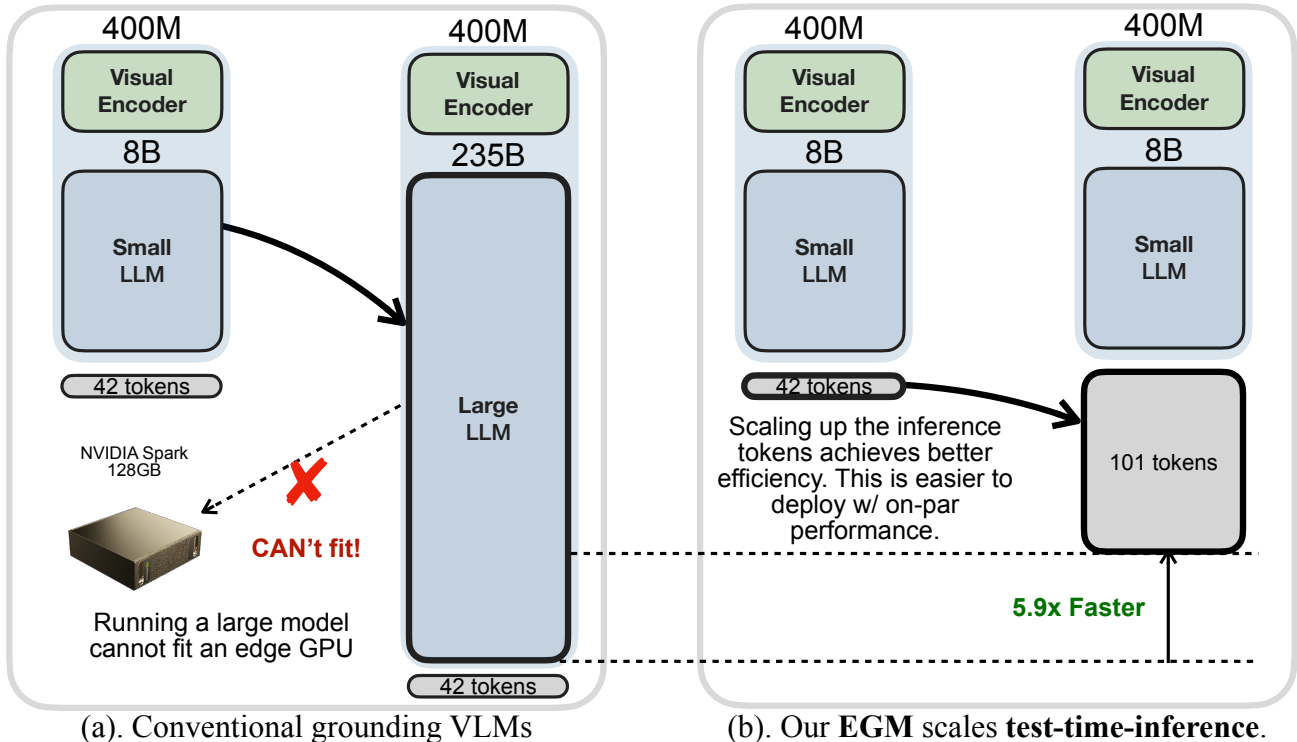


Figure 1. **Overview of test-time scaling for visual grounding.** *Left.* Existing state-of-the-art grounding VLMs usually have large model sizes. *Right.* Our EGM extends scaling laws by scaling up inference tokens to enhance text understanding capabilities of small VLMs, achieving better efficiency.

improve the visual grounding capability of small models and significantly mitigate the gap between small models and bigger models. We name our models ‘*Efficient visual Grounding language Models*’ (EGM).

In summary, we make the following contributions:

- We identify ‘COMPLEX\_PROMPT’ as the main reason why small VLMs lag behind bigger ones. To address this, we introduce EGM, which equips small VLMs with multi-modal reasoning abilities through extended test-time computation to enhance their visual grounding capabilities.
- We prepare SFT and RL data that enables reasoning skills for small VLMs. We also set up data for amodal grounding, which requires the model to predict both visible and occluded parts of the target objects, to further validate our method’s generality.
- Our experiments show that EGM consistently boosts the grounding performance of small VLMs across sizes and model families, in both vanilla and amodal grounding. For example, on the RefCOCO [19, 32] benchmark, our 8B model achieves a 91.4 IoU, beating the 235B model’s 90.5 IoU and running 5.9× faster.

## 2. Related Work

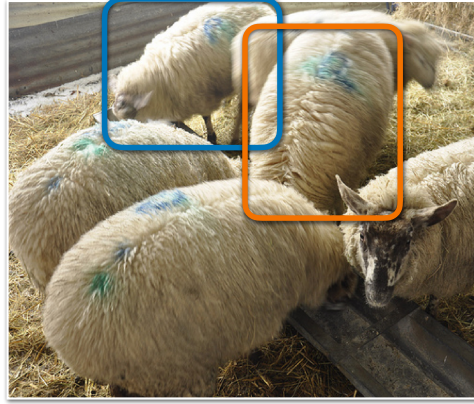
**Visual-Language Models (VLMs)** have advanced rapidly recently. Proprietary ones such as GPT [1, 17], Gemini [11, 37, 38], Claude [3], and Grok [44] have greatly improved performance on specific tasks and capability of multiple modalities. On the other hand, open-source VLMs have also developed continuously, closing the gap between open-source and proprietary models. Representative examples include Qwen [5, 6, 41], InternVL [9, 42, 51], LLaVA [22], Llama [13, 39, 40], VILA [28, 30] and Molmo [12]. The main architecture of these models is LLaVA-like, *i.e.*, the image is firstly fed into a ViT encoder, and then projected to the LLM via an MLP.

**Grounding VLMs.** Visual grounding lets VLMs predict a bounding box for a target object given a text prompt. This is a fundamental capability of VLMs to understand the visual world. Leading open-source models, such as InternVL [42] and Qwen [6], perform best on the RefCOCO [19, 32] benchmark, even surpassing proprietary models such as GPT [17] and Gemini [11].

Beyond the standard grounding task, *amodal grounding*, where the model predicts a box covering both the visible and hidden parts of the target described in the prompt,



**Text Prompt:** chair **empty next to** guy  
**Error Cause:** relative descriptions



**Text Prompt:** Farthest sheep **close to** metal  
**Error Cause:** spatial relationship

 : Ground Truth  
 : Prediction from small VLMs



**Text Prompt:** **Tall man watch** cutting cake  
**Error Cause:** compositional reasoning



**Text Prompt:** The **empty part** of the blue plate **on the left**  
**Error Cause:** spatial relationships + compositional reasoning

Figure 2. **Failure cases of small VLMs.** We find small VLMs, e.g., InternVL-3-8B, tend to fail when the text prompt is *semantically complicated* and there are *multiple candidates* in the image that can confuse the model. We term this failure pattern ‘COMPLEX\_PROMPT’ and label the ground truth bbox in blue, and the 8B model prediction in orange in examples.

is also gaining increasing attention. This ‘amodal’ ability reflects how humans perceive objects as complete, even when occluded [7, 18], and benefits real-world tasks like autonomous driving and robotics [48]. Although amodal completion is gaining attention in computer vision [4, 8, 10, 16, 23–27, 29, 31, 33, 43, 46, 48, 50, 52, 53], VLMs have not mastered this skill, even for the most advanced proprietary models. In this paper, we are the first to study *amodal grounding* in VLMs, aiming to boost their amodal grounding ability as well as the efficiency.

**Reasoning.** Reasoning has become a critical capability of modern LLMs, supporting key applications such as mathematical problem solving and code generation. Guo et al. [15] introduced an effective reasoning-training pipeline that combined a SFT cold start with Group Relative Policy Optimization (GRPO) [34], showing that structured reasoning traces together with reward optimization can substantially improve a model’s reasoning ability. Following this line

of work, a series of GRPO-style algorithms have been proposed. Yu et al. [47] developed Dynamic Sampling Policy Optimization (DAPO), which used a token-level mean loss to enable importance sampling and advantage estimation at the token granularity. Tan et al. [36] further introduced Group Token Policy Optimization (GTPO), which incorporated entropy regularization into the GRPO framework to encourage more diverse model responses.

### 3. Why Small VLMs Fall Behind?

We start with the InternVL series of models. On RefCOCO benchmarks, we randomly select a subset and visualize the predictions from the 8B VLM alongside the ground truth bounding boxes. Following previous work [6, 42, 51], we define a case  $d_i$  as successful if the Intersection-over-Union (IoU) between the bounding box predicted by the model  $M_\theta$  and the ground truth is higher than 0.5. To this end, we

Model	Acc
InternVL-3-8B	0
InternVL-3-32B	29.9%
InternVL-3-78B	42.6%
Gemini-2.5-Pro	22.1%
Gemini-2.5-Flash	20.9%
EGM-InternVL-3-8B	42.7%

Table 1. **Analysis of failure case of ‘COMPLEX\_PROMPT’.** We report the performance of different models on the subset of ReCOCO benchmarks where the InternVL-3-8B model fails due to ‘COMPLEX\_PROMPT’. ‘Acc’ means the ratio of ‘grounding success’ cases. As the model size grows, such failure cases are largely resolved. Our EGM-InternVL-3-8B resolves 42.7% of such failure cases, validating the effectiveness of our method.

define a *grounding success* function:

$$S_{\theta,i} = \begin{cases} 1, & \text{if IoU}_{\theta,i} > 0.5, \\ 0, & \text{otherwise.} \end{cases}, \quad (1)$$

We observe that a large proportion of the failure cases of the small VLM are due to ‘COMPLEX\_PROMPT’: the text prompt is semantically complex and there are multiple similar candidates in the image, so the model mis-locates to another candidate rather than the target object. For example, in the top left example of Figure 2, the model correctly understands the semantics of “chair”, but ignores the instructions “empty” and “next to guy”.

To further verify, we collect a set of failure cases and analyze how these cases improve with model size. Specifically, we select the failure cases from the 8B predictions then send these images together with ground truth to GPT-4, and ask it to analyze the reason for all failure cases where the IoU between the prediction and ground truth boxes is lower than 0.5. The detailed prompt to GPT-4 is provided in Appendix D, where we categorize the failure cases into five categories, such as ‘COMPLEX\_PROMPT’, ‘AMBIGUOUS\_IMAGE’, etc. The result shows that, among all failure cases, 62.8% are due to ‘COMPLEX\_PROMPT’, which confirms our observation.

We further compare with the predictions of bigger models and find that the ‘COMPLEX\_PROMPT’ failure cases of the 8B model can be gradually resolved as the model size grows, as shown in Rows 2 and 3 of Table 1. This motivates us to introduce reasoning to small models to mitigate the gap in understanding ‘COMPLEX\_PROMPT’ compared to bigger models.

## 4. Method

This section presents our method to equip small models with multi-modal reasoning capability through extended

test-time computation. More specifically, we train the model using SFT as the starting point, followed by RL training [15]. We describe the data curation for SFT in Section 4.1, the data curation for RL in Section 4.2, and the training pipeline in Section 4.3. Beyond the standard vanilla grounding task, we extend our method to the amodal grounding, where the model must predict bounding boxes covering both visible and occluded regions of the target objects. Statistics of the curated training datasets are summarized in Table 2. We use proprietary VLMs in the data curation pipeline, and the corresponding prompts are provided in the Appendix B.

### 4.1. SFT Data Curation

The objective of the SFT training stage is to teach the model to learn the reasoning pattern in grounding tasks. As analyzed in Section 3, addressing the key failure pattern requires reasoning about the key feature that distinguishes the target from other objects.

**Vanilla Grounding.** Given an off-the-shelf vanilla grounding training dataset  $\mathcal{D}_G = \{d_i\}_{i=1}^N$ , each sample  $d_i$  contains an image, a textual query, and the corresponding ground-truth bounding box. We present each  $d_i$  to a proprietary VLM  $\Phi$  (e.g., GPT-4 [17]) to obtain its reasoning trace:

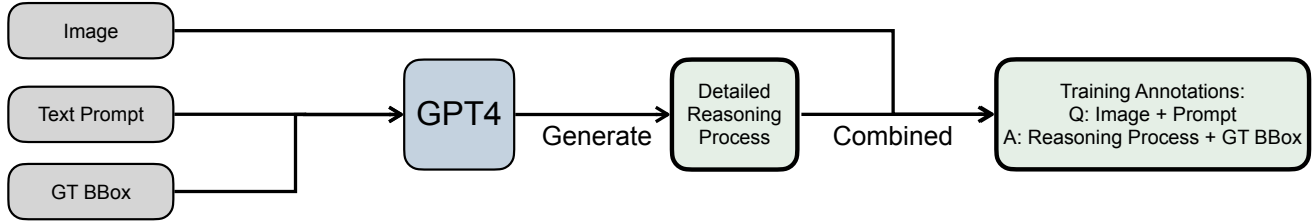
$$z_i = \Phi(d_i). \quad (2)$$

We then pair each original sample  $d_i$  with its reasoning trace  $z_i$  to obtain the reasoning training dataset  $\mathcal{D}_C = \{(d_i, z_i)\}_{i=1}^N$ . Dataset statistics for  $\mathcal{D}_G$  and  $\mathcal{D}_C$  are reported in Table 2 as the vanilla grounding category.

An example of vanilla grounding is shown on the bottom left of Figure 3. For the text prompt ‘vase with handle’, the answer involves a reasoning process that analyzes the distinct feature of the target vase compared with others.

**Amodal Grounding.** Unlike vanilla grounding, there is no off-the-shelf data for training that provides both the text prompt and the corresponding amodal bounding box. To bridge the gap, we use a proprietary VLM to generate a more detailed description of the target object that can uniquely specify it in the existing amodal segmentation datasets, such as COCO-Amodal [52] and TAO-Amodal [16]. We further conduct a verification step on the generated prompts to remove the noisy ones. We denote the generated dataset so far as  $\mathcal{D}_T$ .

Once we obtain the text prompt associated with the amodal bounding box, we generate the reasoning process via the same pipeline as introduced for vanilla grounding. The only difference is that, in addition to locating the target object, the reasoning should also involve: 1) what object(s) are causing the occlusion; 2) what this object’s complete unoccluded shape looks like; 3) in which direction(s) and how much the visible parts should be extended to recover the complete object. An example of generated reasoning



(a). Our data curation pipeline



(b). Visualized examples of curated data

Figure 3. **Overview of our method.** *Top (a): Data curation pipeline of training data with reasoning.* We feed the image, text prompt and ground truth bounding box of the target object into a proprietary VLM to generate the detailed reasoning process of how to locate the object correctly given the image and text prompt. The generated reasoning process is incorporated as part of the training data. *Bottom (b): Examples of generated reasoning training data for vanilla grounding and amodal grounding.* The reasoning process of vanilla grounding analyzes the feature that distinguishes the target object from others, and the reasoning process of amodal grounding further involves what object causes the occlusion and in which directions the visible parts should be extended to recover the complete object.

Category	#Samples	#Images	Avg. #BBoxes	Width	Height
Vanilla Grounding	575,208	24,407	2.3 $\pm$ 1.3	585.7 $\pm$ 87.0	480.3 $\pm$ 93.1
Amodal Grounding	23,698	15,798	1.5 $\pm$ 1.5	1186.2 $\pm$ 332.0	717.2 $\pm$ 175.2

Table 2. **Statistics of curated training datasets** for vanilla grounding and amodal grounding. The vanilla grounding category is for the vanilla grounding training dataset  $\mathcal{D}_G$  and the vanilla grounding reasoning training dataset  $\mathcal{D}_C$  curated from RefCOCO training dataset [30]. The amodal grounding category is for the amodal grounding training dataset  $\mathcal{D}_T$  and amodal grounding reasoning training dataset  $\mathcal{D}_A$  curated from COCO-Amodal [52] and TAO-Amodal [16].

data for amodal grounding is shown on the bottom right of Figure 3. The question is to predict the amodal bounding box of the tiger behind the fallen log on the right. The reasoning process thus involves ‘the fallen log in front is causing the occlusion’, ‘the complete shape of the tiger includes its full torso, legs, and tail’, and ‘to recover the full object, extend downward from the visible part considerably’. This process yields the final amodal grounding dataset with reasoning  $\mathcal{D}_A$ . Additional details are provided in Appendix B.

## 4.2. RL Data Curation

**Vanilla Grounding.** We select a harder subset of the off-the-shelf vanilla grounding training dataset  $\mathcal{D}_G = \{d_i\}_{i=1}^N$  in Table 2 for vanilla grounding RL training by learnability [14, 49]. More specifically, given the learner model  $M_\theta$  and the reference model  $M_{\text{ref}}$ , we first compute their IoU values on the entire training dataset  $\mathcal{D}_G$ . The learnability of each sample  $d_i$  is calculated as  $l_i = S_{\text{ref},i} - S_{\theta,i}$ . The

learner model is a small VLM that we train, and the reference model is a state-of-the-art visual grounding model.

For each learner model, we then construct a negative sample set  $\mathcal{D}_{\text{neg}} = \{d_i \mid l_i > 0, d_i \in \mathcal{D}_G\}$ , where the learnability is greater than 0. Next, we uniformly sample instances with  $S_{\theta,i} = 1$  from  $\mathcal{D}_G$  to form a positive sample set  $\mathcal{D}_{\text{pos}}$  of equal size to  $\mathcal{D}_{\text{neg}}$ . The final training dataset is the union of the two subsets:  $\mathcal{D} = \mathcal{D}_{\text{pos}} \cup \mathcal{D}_{\text{neg}}$ . The motivation for this is that we want to select harder samples for RL training to enable the model to learn the grounding capability, but we don’t want to overfit only on hard samples, so we also mix in some positive samples.

**Amodal Grounding.** We use the entire amodal grounding dataset  $\mathcal{D}_T$  in Table 2 to make the most of the limited data and to strengthen the model’s performance in this new task.

### 4.3. Training Pipeline and Reward

**Training Pipeline.** We first perform SFT on the base model so that the model learns the desired reasoning pattern. Subsequently, we further train the model using reinforcement learning to obtain the final EGM models. We adopt the GRPO [34] with a token-level mean loss [47]. The KL divergence penalty and the entropy regularization are introduced to ensure that the model maintains sufficient exploration during reasoning while avoiding pattern collapse.

Specifically, for a given input  $q$  and its  $i$ -th generated sequence  $o_i$  sampled from the behavior policy  $\pi_{\theta_{\text{old}}}$ , we denote its length by  $|o_i|$  and its token sequence as  $\{o_{i,t}\}_{t=1}^{|o_i|}$ . The overall GRPO objective is defined as:

$$\begin{aligned} \mathcal{J}_{\text{GRPO}}(\pi_{\theta}) &= \mathbb{E}_{q \sim P(Q), \{o_i\}_{i=1}^G \sim \pi_{\theta_{\text{old}}}(O|q)} \quad (3) \\ & \left[ \frac{1}{G} \sum_{i=1}^G \sum_{t=1}^{|o_i|} \min \left( \frac{\pi_{\theta}(o_{i,t} | q, o_{i,<t})}{\pi_{\theta_{\text{old}}}(o_{i,t} | q, o_{i,<t})} \hat{A}_{i,t}, \right. \right. \\ & \quad \left. \left. \text{clip} \left( \frac{\pi_{\theta}(o_{i,t} | q, o_{i,<t})}{\pi_{\theta_{\text{old}}}(o_{i,t} | q, o_{i,<t})}, 1 - \epsilon, 1 + \epsilon \right) \hat{A}_{i,t} \right) \right. \\ & \quad \left. - \beta \mathbb{D}_{\text{KL}}(\pi_{\theta} \parallel \pi_{\text{ref}}) + \gamma \mathbb{H}(\pi_{\theta}) \right], \quad (4) \end{aligned}$$

$$\mathbb{D}_{\text{KL}}(\pi_{\theta} \parallel \pi_{\text{ref}}) = \frac{\pi_{\text{ref}}(o_i | q)}{\pi_{\theta}(o_i | q)} - \log \frac{\pi_{\text{ref}}(o_i | q)}{\pi_{\theta}(o_i | q)} - 1, \quad (5)$$

$$\mathbb{H}(\pi_{\theta}) = -\log \pi_{\theta}(o_i | q), \quad (6)$$

where  $\beta$  and  $\gamma$  are hyper-parameters;  $\epsilon$  is PPO clip ratio;  $\pi_{\text{ref}}$  is the reference model; and  $\hat{A}_{i,t}$  is the token level advantage, derived from the rewards  $\{r_1, r_2, \dots, r_G\}$  corresponding to the outputs within each group:

$$\hat{A}_i = \frac{r_i - \text{mean}(\{r_j\}_{j=1}^G)}{\text{std}(\{r_j\}_{j=1}^G)}, \hat{A}_{i,t} = \hat{A}_i / |o_i|. \quad (7)$$

**Reward.** We define the reward as a weighted combination of localization accuracy and *grounding success* with hyper-parameter  $\alpha$ :

$$r_i = \alpha \text{IoU}_{\theta,i} + (1 - \alpha) S_{\theta,i}. \quad (8)$$

The  $\alpha$  is set to 0.5 by default during experiments unless specifically clarified.

## 5. Experiments

### 5.1. Implementation Details

**Models.** We apply our method to the state-of-the-art visual grounding open-source VLM families InternVL and QwenVL, and add a prefix ‘EGM-’ to models to which our method has been applied. Our experiments are conducted on InternVL-3-1B, InternVL-3-2B and InternVL-3-8B for

the InternVL family, and on Qwen3-VL-2B-Thinking, Qwen3-VL-4B-Thinking and Qwen3-VL-8B-Thinking for the QwenVL family.

**SFT.** For the SFT training stage, we use the official GitHub scripts of InternVL-3 and Qwen3-VL. The training dataset statistics are presented in Table 2. The learning rate is set to be  $1e - 5$ , the epoch is set to be 1 and the training batch size is 128. We train all models on 8 A100 GPUs.

**RL.** For the reinforcement learning stage, we employ the VeRL framework [35]. All rollouts and inference are performed using the vLLM engine [21]. We train with a learning rate of  $3e - 6$  for 5 epochs and a batch size of 256. The reward weight  $\alpha$  in Equation 8 is fixed to 0.5. For the Qwen model series, we set the KL coefficient to  $\beta = 0.005$  and the entropy coefficient to  $\gamma = 0.0$ . For the InternVL model series, we use  $\beta = 0.0$  and  $\gamma = 0.01$ . We construct the RL training dataset following the procedure described in Section 4.2, using InternVL-3.5-241B as the reference model  $M_{\text{ref}}$  and the corresponding fine-tuned model as  $M_{\theta}$ . The final dataset size varies across models. We present details of RL training dataset samples, and full details about hyper-parameters of RL training and rollout in Appendix A.1.

### 5.2. Evaluation Benchmarks and Metrics

**Vanilla Grounding Benchmark.** For vanilla grounding, we use the standard RefCOCO [19, 32] benchmarks for evaluation, which contain eight test splits. We adopt ‘accuracy’ as the evaluation metric, *i.e.*, the proportion of *grounding success*  $S_{\theta,i}$  as defined in Equation 1. We report the score on individual splits as well as the average score over the eight splits.

**Amodal Grounding Benchmark.** As there is no off-the-shelf benchmark for amodal grounding, we start from the standard amodal benchmark in the computer vision community – the val and test splits of COCO-Amodal [52] dataset, and use the pipeline as introduced in Section 4.1 to generate text prompts. We therefore obtain an evaluation benchmark consisting of 11,261 samples and 2,474 images. We adopt the same evaluation metric as vanilla grounding.

**Efficiency Metric.** To measure efficiency, besides the number of model parameters, we also calculate the average latency per sample on a random 10% subset of the standard RefCOCO benchmarks for evaluation. Latency is measured as the time (in milliseconds) from sending the text prompt to receiving the entire answer from the model. For models that cannot be deployed on a single GPU, we run inference on them with multiple GPUs. Therefore, for fair comparison, we report *GPU latency* in practice, which is the product of latency and number of GPUs. We measure latency on the same L20 GPUs.

We adopt identical inference hyper-parameters for all models during evaluation. The only differences in the

Model	RefCOCO			RefCOCO+			RefCOCOg		Avg. Acc
	val	test-A	test-B	val	test-A	test-B	val	test	
Qwen3-VL-2B-Instruct	88.7	90.8	84.7	80.1	85.7	73.1	84.8	85.7	84.2
Qwen3-VL-2B-Thinking	87.5	91.4	82.0	80.2	86.7	72.1	84.4	84.5	83.6
+ EGM	93.0	94.0	89.4	87.8	91.7	82.7	88.6	89.3	89.6 <sup>+6.0↑</sup>
Qwen3-VL-4B-Instruct	91.0	92.7	87.6	84.4	88.7	78.2	88.3	87.8	87.3
Qwen3-VL-4B-Thinking	90.0	92.7	85.6	85.2	89.5	79.3	87.8	87.7	87.2
+ EGM	93.5	95.1	90.9	89.7	93.1	84.9	90.4	90.8	91.0 <sup>+3.8↑</sup>
Qwen3-VL-8B-Instruct	91.6	93.3	87.8	85.8	90.3	79.9	88.7	88.7	88.3
Qwen3-VL-8B-Thinking	91.0	92.9	86.9	86.2	89.3	80.2	87.6	88.6	87.8
+ EGM	93.9	95.0	91.2	90.1	93.3	85.9	90.4	91.2	91.4 <sup>+3.6↑</sup>
Qwen3-VL-235B-A22B-Instruct	92.9	94.6	90.2	88.6	92.4	84.2	90.3	90.8	90.5
Qwen3-VL-235B-A22B-Thinking	92.9	94.1	90.6	89.5	92.5	85.5	90.4	90.5	90.7
InternVL-3-1B	85.8	90.1	81.7	76.6	84.1	69.2	82.8	82.6	81.6*
+ EGM	90.2	93.2	87.0	83.8	88.8	77.5	86.4	87.5	86.8 <sup>+5.2↑</sup>
InternVL-3-2B	89.8	92.6	86.4	84.0	89.2	76.5	87.6	87.2	86.7*
+ EGM	92.2	94.0	87.4	85.6	91.2	79.2	88.5	88.7	88.4 <sup>+1.7↑</sup>
InternVL-3-8B	92.5	94.6	88.0	88.2	92.5	81.8	89.6	90.0	89.6*
+ EGM	93.6	95.2	90.1	89.3	93.6	83.1	89.7	90.7	90.7 <sup>+1.1↑</sup>
InternVL-3-78B	93.4	95.4	90.3	90.1	93.8	85.3	91.5	91.5	91.4*
Gemini-2.5-Pro	66.8	66.8	69.2	58.2	58.2	60.6	65.0	65.7	63.8
GPT-5	42.6	46.0	39.3	37.4	40.1	35.2	39.1	41.0	40.1

Table 3. **Accuracy results for vanilla grounding.** Our method consistently improves the performance of models of different sizes and from different families. Entries marked with \* are from the official report [42], and the others are measured by ourselves.

prompts follow the model-family-specific formats prescribed in the official implementation. Further details of the evaluation setup are provided in Appendix A.2.

### 5.3. Vanilla Grounding

Table 3 shows the results of applying our method to models of different sizes from the InternVL-3 family and the Qwen3-VL family.

**EGM consistently improves the grounding performance.** EGM boosts the performance of Qwen3-VL-2B/4B/8B-Thinking by +5.5/+3.7/+3.6 and InternVL-3-1B/2B/8B by +4.9/+1.7/+1.1 for the average accuracy. This shows the generality of our EGM that can improve small VLMs of *different sizes* and from *different families* on RefCOCO benchmarks.

**EGM can mitigate the gap between small models and larger models.** For example, the performance of Qwen3-VL-2B/4B/8B-Thinking is 83.6/87.2/87.8. Our 2B and 4B

models outperform Qwen3-VL-8B-Thinking by +1.3/+3.1. Our EGM shows that scaling the test-time computation can boost the performance by improving text understanding.

**Our reasoning is faster and more accurate than Qwen3-VL-Thinking.** For the Qwen3-VL models, 2B/4B/8B-Thinking does not outperform 2B/4B/8B-Instruct (-0.6/-0.1/-0.5), but our 2B/4B/8B reasoning models significantly outperform 2B/4B/8B-Instruct (+4.9/+3.6/+3.1), demonstrating the effectiveness of our multi-modal reasoning.

### 5.4. Amodal Grounding

To further verify the effectiveness of our method, we show the accuracy results on the new task of amodal grounding in Table 4. Similar to vanilla grounding, **our method consistently boosts the performance of models of different sizes and from different families** by +7.4/+6.4/+11.5 (InternVL-3) and +6.9/+2.3/+2.5 (Qwen3-VL), demonstrating the wide applicability of our method for different tasks.

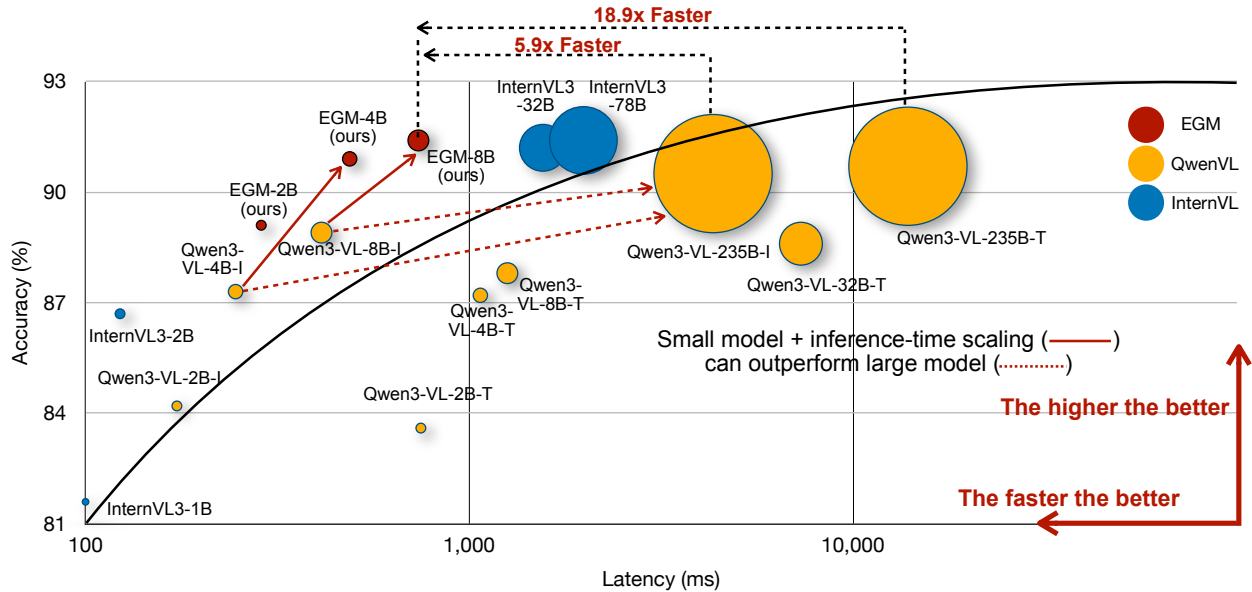


Figure 4. **Accuracy vs. Efficiency.** Our models, EGM-Qwen3-VL-2B, EGM-Qwen3-VL-4B and EGM-Qwen3-VL-8B, have greatly improved the efficiency of visual grounding. For example, EGM-Qwen3-VL-8B outperforms both the state-of-the-art Qwen3-VL-235B-Instruct and Qwen3-VL-235B-Thinking models for accuracy, while speeding up  $5.9\times/18.9\times$  in terms of GPU latency. For Qwen models, ‘-T’ denotes ‘-Thinking’ and ‘-I’ denotes ‘-Instruct’.

Model	Amodal Acc
InternVL3-1B	56.9
+ EGM	64.3 <sup>+7.4↑</sup>
InternVL3-2B	63.8
+ EGM	70.2 <sup>+6.4↑</sup>
InternVL3-8B	62.0
+ EGM	73.5 <sup>+11.5↑</sup>
InternVL3-38B	36.0
InternVL3-78B	51.0
Qwen3-VL-2B-Thinking	66.5
+ EGM	73.4 <sup>+6.9↑</sup>
Qwen3-VL-4B-Thinking	71.6
+ EGM	73.9 <sup>+2.3↑</sup>
Qwen3-VL-8B-Thinking	71.4
+ EGM	73.9 <sup>+2.5↑</sup>
Qwen3VL-32B-Instruct	74.4
Qwen3VL-32B-Thinking	73.6
Qwen3VL-235B-A22B-Instruct	74.6
Qwen3VL-235B-A22B-Thinking	74.1
Gemini-2.5-Pro	52.3
GPT-5	24.7

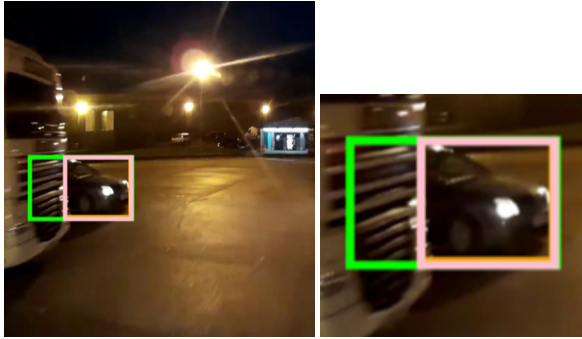
Table 4. **Accuracy results for amodal grounding.** Similar to vanilla grounding, our method consistently boosts the performance of amodal grounding.

Moreover, in Figure 5 we show demos of our EGM models in autonomous driving and robotics scenarios. The top left demo is a situation called ‘ghost probe’, where a car crossing the road suddenly appears. In this situation, it is important to notice and figure out the complete shape of the occluded car when they have not fully appeared. The top right demo for robotics is collected from the DROID dataset [20]. In this situation, the robot arm is going to manipulate the objects on the table and it is important to know the complete shape of occluded objects, *e.g.*, the pen, for robust manipulation, as discussed in [45]. The bottom demos are two additional demos for driving scenario. For all cases, it can be observed that compared with Qwen3-VL-8B and Qwen3-VL-235B, our EGM-Qwen3-VL-8B can reason about the occlusion situations and correctly predict the complete shape of the occluded pedestrian, the occluded car and the occluded pen. This suggests the potential application of our EGM models in autonomous driving and robotic manipulation tasks.

### 5.5. Efficiency Comparison

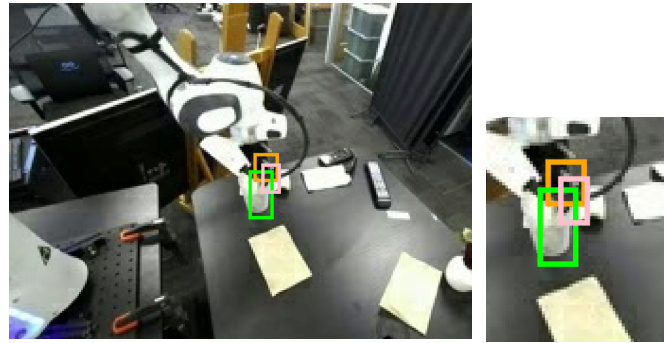
Figure 4 compares the accuracy and efficiency of models in the QwenVL family. **Our EGM models significantly improve the efficiency of visual grounding:** Both our 4B and 8B models surpass the 235B models in accuracy and are over  $5\times$  faster in inference. Our 2B model also outperforms several larger models—32B-Thinking, 8B-Instruct, and 8B-Thinking—while achieving better GPU latency. The observation is consistent with the results in Table 3, demonstrat-

Qwen3-VL-8B (Orange)
  EGM-Qwen3-VL-8B (Green)
  Qwen3-VL-235B (Pink)



**Text Prompt:** the black car crossing the road

**EGM Reasoning:** The black car is located near the left edge of the image, partially crossing the road. The white truck on the left is blocking part of the car. The car's full shape is a typical sedan, with the left side hidden behind the truck. To recover the complete car, extend its visible part significantly to the left. No other objects are causing occlusion.



**Text Prompt:** pen in the cup

**EGM Reasoning:** The pen is located inside the white cup on the table near the center of the image. The cup is causing the occlusion, hiding the lower part of the pen. The complete shape of the pen is a long, thin cylinder extending downward into the cup. To recover the full object, extend the visible part significantly downward. No other objects are causing occlusion.



**Text Prompt:** the silver sedan with a "corolla" badge

**EGM Reasoning:** The silver sedan with a "corolla" badge is directly ahead in the center of the image, identifiable by its rear emblem and license plate. The lower part of the car is blocked by the dashboard or windshield frame of the vehicle from which the photo is taken. The complete shape includes the full rear bumper and wheels, which are not visible. To recover the full object, extend downward moderately from the visible part. No other directions need expansion.



**Text Prompt:** the man in a red shirt on the left

**EGM Reasoning:** The man in a red shirt on the left can be found walking across the street near the bottom left of the image. His lower legs and feet are blocked by the dashboard of the car from which the photo was taken. His full shape includes his head, torso, arms, and legs down to his shoes. To recover the complete object, extend downward a bit from the visible part to include his feet. No other objects besides the car dashboard are causing the occlusion.

Figure 5. **Demo** of Qwen3-VL-8B, Qwen3-VL-235B, and our EGM-Qwen3-VL-8B for amodal grounding on autonomous driving and robotics scenarios.

ing the effectiveness of extending scaling laws through test-time computation for visual grounding.

## 5.6. Qualitative Comparison

Figure 6 shows the qualitative comparison of Qwen3-VL-8B, Qwen3-VL-235B, and our EGM-Qwen3-VL-8B for vanilla grounding and amodal grounding. Please refer to Appendix C for more qualitative results.

The top left, top right and bottom left samples are vanilla grounding on RefCOCO benchmark. For the *top left* example, the text prompt is 'girl third from right front row', and the Qwen3-VL-8B model mis-locates to the 'second' girl. Our EGM-Qwen3-VL-8B correctly reasons the key

feature 'count the individuals from the rightmost person in the front row, moving left' and generates a correct prediction. For the *top right* example, the text prompt is 'chair next to striped chair', and the Qwen3-VL-8B model confuses it with the striped chair itself. Our EGM-Qwen3-VL-8B, however, correctly reasons about the key feature 'the chair that is positioned next to a striped chair' and outputs the correct grounding box. For the *bottom left* example, the text prompt is 'boy touching light bat', and the Qwen3-VL-8B model fails to understand 'touching light bat' and mis-predicts the boy touching the darker bat. Our EGM-Qwen3-VL-8B predicts the correct boy, with a reasoning that it should be 'the individual whose hand is in contact



**Text Prompt:** girl third from right front row

**EGM Reasoning:** To identify the "girl third from right front row," count the individuals from the rightmost person in the front row, moving left. The third person in this sequence is the target, and the bounding box should encompass this individual accurately.



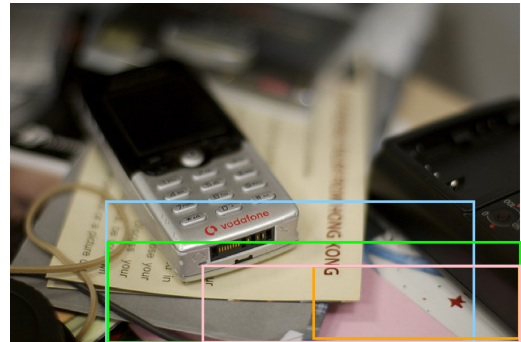
**Text Prompt:** boy touching light bat

**EGM Reasoning:** To correctly identify the target object, focus on the boy who is physically interacting with a light-colored bat. Look for the individual whose hand is in contact with the bat, ensuring the bat's color matches the description, and verify that the boy is distinct from others who may be holding or near similar objects.



**Text Prompt:** chair next to striped chair

**EGM Reasoning:** To correctly identify the target object, locate the chair that is positioned next to a striped chair. Focus on the spatial relationship described, ensuring the selected chair is adjacent to the striped one, which helps distinguish it from other similar objects in the scene.



**Text Prompt:** the pink paper partially covered by a cellphone

**EGM Reasoning:** The pink paper is located beneath the silver cellphone, with only a small portion visible. The cellphone is causing the occlusion. The complete shape of the pink paper is rectangular, extending further to the left and upward beyond what is visible. To recover the full object, expand considerably to the left and significantly to the top from the visible part. The rest of the paper is likely hidden under the cellphone and possibly other objects.

Figure 6. **Qualitative comparison** of Qwen3-VL-8B, Qwen3-VL-235B, and our EGM-Qwen3-VL-8B for vanilla grounding and amodal grounding. Vanilla grounding: top left, top right and bottom left; Amodal grounding: bottom right.

with the bat, ensuring the bat's color matches the description'. For the vanilla grounding cases, generally Qwen3-VL-235B performs better than Qwen3-VL-8B, as can be observed in the examples.

The *bottom right* example is amodal grounding on the COCO-Amodal benchmark. It can be observed that Qwen3-VL-8B and Qwen3-VL-235B fail to predict the amodal grounding box of 'the pink paper partially covered

by a cellphone’, while our EGM-Qwen3-VL-8B prediction is close to the ground truth, with reasoning process about locating the pink paper, analyzing it is occluded by the cellphone and other objects and should extend to the left and upward to recover the full unoccluded shape. This reasoning helps EGM-Qwen3-VL-8B to better locate the amodal bounding box covering both the visible and occluded parts of the pink paper.

## 6. Conclusion

In this paper, we introduced ‘Efficient visual Grounding language Models’ (EGM), a method to improve the efficiency of visual grounding language models. Our method equips small models with the multi-modal reasoning capability through extended test-time computation, via a two-stage SFT-RL training paradigm. Experiments show our method can be applied to different model families, different model sizes, and different tasks, to boost the performance consistently and significantly. Therefore, our EGM achieves a 91.4 IoU with an 8B model, outperforming the conventional 235B model with a 90.5 IoU, while speeding up  $5.9\times$ . We hope systems developed in this way can help scenarios such as autonomous driving and robotics, where an efficient grounding language model with amodal capability is important.

**Acknowledgments.** We thank Prof. Andrew Zisserman, An-Chieh Cheng, Haiyan Huang, Sifei Liu, Baifeng Shi, Hongxu Yin, Hanrong Ye, Wenwei Zhang for their suggestions, help and support for the project.

## References

- [1] Josh Achiam, Steven Adler, Sandhini Agarwal, Lama Ahmad, Ilge Akkaya, Florencia Leoni Aleman, Diogo Almeida, Janko Altmenschmidt, Sam Altman, Shyamal Anadkat, et al. Gpt-4 technical report. *arXiv preprint arXiv:2303.08774*, 2023. 2
- [2] Alibaba. Qwen3-vl, 2025. 1
- [3] Anthropic. Claude-4.5, 2025. 2
- [4] Jiayang Ao, Yanbei Jiang, QiuHong Ke, and Krista A Ehinger. Open-world amodal appearance completion. In *Proceedings of the Computer Vision and Pattern Recognition Conference*, pages 6490–6499, 2025. 3
- [5] Jinze Bai, Shuai Bai, Yunfei Chu, Zeyu Cui, Kai Dang, Xiaodong Deng, Yang Fan, Wenbin Ge, Yu Han, Fei Huang, et al. Qwen technical report. *arXiv preprint arXiv:2309.16609*, 2023. 2
- [6] Shuai Bai, Keqin Chen, Xuejing Liu, Jialin Wang, Wenbin Ge, Sibao Song, Kai Dang, Peng Wang, Shijie Wang, Jun Tang, et al. Qwen2. 5-vl technical report. *arXiv preprint arXiv:2502.13923*, 2025. 1, 2, 3
- [7] Robert Eamon Briscoe. Mental imagery and the varieties of amodal perception. *Pacific Philosophical Quarterly*, 92(2): 153–173, 2011. 3
- [8] Kaihua Chen, Deva Ramanan, and Tarasha Khurana. Using diffusion priors for video amodal segmentation. In *Proceedings of the Computer Vision and Pattern Recognition Conference*, pages 22890–22900, 2025. 3
- [9] Zhe Chen, Jiannan Wu, Wenhai Wang, Weijie Su, Guo Chen, Sen Xing, Muyan Zhong, Qinglong Zhang, Xizhou Zhu, Lewei Lu, et al. Internvl: Scaling up vision foundation models and aligning for generic visual-linguistic tasks. In *Proceedings of the IEEE/CVF conference on computer vision and pattern recognition*, pages 24185–24198, 2024. 2
- [10] Seunggeun Chi, Enna Sachdeva, Pin-Hao Huang, and Kwongjoon Lee. Contact-aware amodal completion for human-object interaction via multi-regional inpainting. In *Proceedings of the IEEE/CVF International Conference on Computer Vision*, pages 9487–9496, 2025. 3
- [11] Gheorghe Comanici, Eric Bieber, Mike Schaekermann, Ice Pasupat, Noveen Sachdeva, Inderjit Dhillon, Marcel Blisstein, Ori Ram, Dan Zhang, Evan Rosen, et al. Gemini 2.5: Pushing the frontier with advanced reasoning, multimodality, long context, and next generation agentic capabilities. *arXiv preprint arXiv:2507.06261*, 2025. 2
- [12] Matt Deitke, Christopher Clark, Sangho Lee, Rohun Tripathi, Yue Yang, Jae Sung Park, Mohammadreza Salehi, Niklas Muennighoff, Kyle Lo, Luca Soldaini, et al. Molmo and pixmo: Open weights and open data for state-of-the-art multimodal models. *arXiv e-prints*, pages arXiv–2409, 2024. 2
- [13] Abhimanyu Dubey, Abhinav Jauhri, Abhinav Pandey, Abhishek Kadian, Ahmad Al-Dahle, Aiesha Letman, Akhil Mathur, Alan Schelten, Amy Yang, Angela Fan, et al. The llama 3 herd of models. *arXiv e-prints*, pages arXiv–2407, 2024. 2
- [14] Talfan Evans, Nikhil Parthasarathy, Hamza Merzic, and Olivier J Henaff. Data curation via joint example selection further accelerates multimodal learning. *Proceedings of the Advances in Neural Information Processing Systems (NeurIPS)*, 2024. 5
- [15] Daya Guo, Dejian Yang, Haowei Zhang, Junxiao Song, Ruoyu Zhang, Runxin Xu, Qihao Zhu, Shirong Ma, Peiyi Wang, Xiao Bi, et al. Deepseek-r1: Incentivizing reasoning capability in llms via reinforcement learning. *arXiv preprint arXiv:2501.12948*, 2025. 3, 4
- [16] Cheng-Yen Hsieh, Tarasha Khurana, Achal Dave, and Deva Ramanan. Tracking any object amodally. *arXiv preprint arXiv:2312.12433*, 2023. 3, 4, 5, 16
- [17] Aaron Hurst, Adam Lerer, Adam P Goucher, Adam Perelman, Aditya Ramesh, Aidan Clark, AJ Ostrow, Akila Welihinda, Alan Hayes, Alec Radford, et al. Gpt-4o system card. *arXiv preprint arXiv:2410.21276*, 2024. 1, 2, 4, 16
- [18] Barbara Kaup, Rolf Ulrich, Karin M Bausenhart, Donna Bryce, Martin V Butz, David Dignath, Carolin Dudschig, Volker H Franz, Claudia Friedrich, Caterina Gawrilow, et al. Modal and amodal cognition: an overarching principle in various domains of psychology. *Psychological Research*, 88(2):307–337, 2024. 3
- [19] Sahar Kazemzadeh, Vicente Ordonez, Mark Matten, and Tamara Berg. Referitgame: Referring to objects in pho-

- tographs of natural scenes. In *Proceedings of the 2014 conference on empirical methods in natural language processing (EMNLP)*, pages 787–798, 2014. 2, 6
- [20] Alexander Khazatsky, Karl Pertsch, Suraj Nair, Ashwin Balakrishna, Sudeep Dasari, Siddharth Karamcheti, Soroush Nasiriany, Mohan Kumar Srirama, Lawrence Yunliang Chen, Kirsty Ellis, Peter David Fagan, Joey Hejna, Masha Itkina, Marion Lepert, Yecheng Jason Ma, Patrick Tree Miller, Jimmy Wu, Suneel Belkhale, Shivin Dass, Huy Ha, Arhan Jain, Abraham Lee, Youngwoon Lee, Marius Memmel, Sungjae Park, Ilija Radosavovic, Kaiyuan Wang, Albert Zhan, Kevin Black, Cheng Chi, Kyle Beltran Hatch, Shan Lin, Jingpei Lu, Jean Mercat, Abdul Rehman, Pannag R Sanketi, Archit Sharma, Cody Simpson, Quan Vuong, Homer Rich Walke, Blake Wulfe, Ted Xiao, Jonathan Heewon Yang, Arefeh Yavary, Tony Z. Zhao, Christopher Agia, Rohan Bajjal, Mateo Guaman Castro, Daphne Chen, Qiuyu Chen, Trinity Chung, Jaimyn Drake, Ethan Paul Foster, Jensen Gao, Vitor Guizilini, David Antonio Herrera, Minh Heo, Kyle Hsu, Jiaheng Hu, Muhammad Zubair Irshad, Donovan Jackson, Charlotte Le, Yunshuang Li, Kevin Lin, Roy Lin, Zehan Ma, Abhiram Maddukuri, Suvir Mirchandani, Daniel Morton, Tony Nguyen, Abigail O’Neill, Rosario Scalise, Derick Seale, Victor Son, Stephen Tian, Emi Tran, Andrew E. Wang, Yilin Wu, Annie Xie, Jingyun Yang, Patrick Yin, Yunchu Zhang, Osbert Bastani, Glen Berseth, Jeannette Bohg, Ken Goldberg, Abhinav Gupta, Abhishek Gupta, Dinesh Jayaraman, Joseph J Lim, Jitendra Malik, Roberto Martín-Martín, Subramanian Ramamoorthy, Dorsa Sadigh, Shuran Song, Jiajun Wu, Michael C. Yip, Yuke Zhu, Thomas Kollar, Sergey Levine, and Chelsea Finn. Droid: A large-scale in-the-wild robot manipulation dataset. 2024. 8
- [21] Woosuk Kwon, Zhuohan Li, Siyuan Zhuang, Ying Sheng, Lianmin Zheng, Cody Hao Yu, Joseph E. Gonzalez, Hao Zhang, and Ion Stoica. Efficient memory management for large language model serving with pagedattention. In *Proceedings of the ACM SIGOPS 29th Symposium on Operating Systems Principles*, 2023. 6
- [22] Bo Li, Yuanhan Zhang, Dong Guo, Renrui Zhang, Feng Li, Hao Zhang, Kaichen Zhang, Peiyuan Zhang, Yanwei Li, Ziwei Liu, et al. Llava-onevision: Easy visual task transfer. *arXiv preprint arXiv:2408.03326*, 2024. 2
- [23] Ke Li and Jitendra Malik. Amodal instance segmentation. In *Proceedings of the European Conference on Computer Vision (ECCV)*, pages 677–693. Springer, 2016. 3
- [24] Zhixuan Li, Weining Ye, Tingting Jiang, and Tiejun Huang. 2d amodal instance segmentation guided by 3d shape prior. In *Proceedings of the European Conference on Computer Vision (ECCV)*, pages 165–181. Springer, 2022.
- [25] Zhixuan Li, Weining Ye, Tingting Jiang, and Tiejun Huang. Gin: Generative invariant shape prior for amodal instance segmentation. *IEEE Transactions on Multimedia (MM)*, 2023.
- [26] Zhixuan Li, Weining Ye, Juan Terven, Zachary Bennett, Ying Zheng, Tingting Jiang, and Tiejun Huang. Muva: A new large-scale benchmark for multi-view amodal instance segmentation in the shopping scenario. In *Proceedings of the IEEE/CVF International Conference on Computer Vision (ICCV)*, pages 23504–23513, 2023.
- [27] Zhenyu Li, Mykola Lavreniuk, Jian Shi, Shariq Farooq Bhat, and Peter Wonka. Amodal depth anything: Amodal depth estimation in the wild. In *Proceedings of the IEEE/CVF International Conference on Computer Vision*, pages 9673–9682, 2025. 3
- [28] Ji Lin, Hongxu Yin, Wei Ping, Pavlo Molchanov, Mohammad Shoeybi, and Song Han. Vila: On pre-training for visual language models. In *Proceedings of the IEEE/CVF conference on computer vision and pattern recognition*, pages 26689–26699, 2024. 2
- [29] Zhaochen Liu, Limeng Qiao, Xiangxiang Chu, Lin Ma, and Tingting Jiang. Towards efficient foundation model for zero-shot amodal segmentation. In *Proceedings of the Computer Vision and Pattern Recognition Conference*, pages 20254–20264, 2025. 3
- [30] Zhijian Liu, Ligeng Zhu, Baifeng Shi, Zhuoyang Zhang, Yuming Lou, Shang Yang, Haocheng Xi, Shiyi Cao, Yuxian Gu, Dacheng Li, et al. Nvila: Efficient frontier visual language models. In *Proceedings of the Computer Vision and Pattern Recognition Conference*, pages 4122–4134, 2025. 2, 5
- [31] Ruijie Lu, Yixin Chen, Yu Liu, Jiayang Tang, Junfeng Ni, Diwen Wan, Gang Zeng, and Siyuan Huang. Taco: Taming diffusion for in-the-wild video amodal completion. In *Proceedings of the IEEE/CVF International Conference on Computer Vision*, pages 13638–13650, 2025. 3
- [32] Junhua Mao, Jonathan Huang, Alexander Toshev, Oana Camburu, Alan L Yuille, and Kevin Murphy. Generation and comprehension of unambiguous object descriptions. In *Proceedings of the IEEE conference on computer vision and pattern recognition*, pages 11–20, 2016. 2, 6
- [33] Ege Ozguroglu, Ruoshi Liu, Dídac Surís, Dian Chen, Achal Dave, Pavel Tokmakov, and Carl Vondrick. pix2gestalt: Amodal segmentation by synthesizing wholes. *Proceedings of the IEEE/CVF Conference on Computer Vision and Pattern Recognition (CVPR)*, 2024. 3
- [34] Zhihong Shao, Peiyi Wang, Qihao Zhu, Runxin Xu, Junxiao Song, Xiao Bi, Haowei Zhang, Mingchuan Zhang, Y. K. Li, Y. Wu, and Daya Guo. Deepseekmath: Pushing the limits of mathematical reasoning in open language models, 2024. 3, 6
- [35] Guangming Sheng, Chi Zhang, Zilingfeng Ye, Xibin Wu, Wang Zhang, Ru Zhang, Yanghua Peng, Haibin Lin, and Chuan Wu. Hybridflow: A flexible and efficient rlhf framework. *arXiv preprint arXiv: 2409.19256*, 2024. 6
- [36] Hongze Tan, Jianfei Pan, Jinghao Lin, Tao Chen, Zhihang Zheng, Zhihao Tang, and Haihua Yang. Gtpo and grpo-s: Token and sequence-level reward shaping with policy entropy, 2025. 3
- [37] Gemini Team, Rohan Anil, Sebastian Borgeaud, Jean-Baptiste Alayrac, Jiahui Yu, Radu Soricut, Johan Schalkwyk, Andrew M Dai, Anja Hauth, Katie Millican, et al. Gemini: a family of highly capable multimodal models. *arXiv preprint arXiv:2312.11805*, 2023. 2
- [38] Gemini Team, Petko Georgiev, Ving Ian Lei, Ryan Burnell, Libin Bai, Anmol Gulati, Garrett Tanzer, Damien Vincent,

- Zhufeng Pan, Shibo Wang, et al. Gemini 1.5: Unlocking multimodal understanding across millions of tokens of context. *arXiv preprint arXiv:2403.05530*, 2024. 2
- [39] Hugo Touvron, Thibaut Lavril, Gautier Izacard, Xavier Martinet, Marie-Anne Lachaux, Timothée Lacroix, Baptiste Rozière, Naman Goyal, Eric Hambro, Faisal Azhar, et al. Llama: Open and efficient foundation language models. *arXiv preprint arXiv:2302.13971*, 2023. 2
- [40] Hugo Touvron, Louis Martin, Kevin Stone, Peter Albert, Amjad Almahairi, Yasmine Babaei, Nikolay Bashlykov, Soumya Batra, Prajjwal Bhargava, Shruti Bhosale, et al. Llama 2: Open foundation and fine-tuned chat models. *arXiv preprint arXiv:2307.09288*, 2023. 2
- [41] Peng Wang, Shuai Bai, Sinan Tan, Shijie Wang, Zhihao Fan, Jinze Bai, Keqin Chen, Xuejing Liu, Jialin Wang, Wenbin Ge, et al. Qwen2-vl: Enhancing vision-language model’s perception of the world at any resolution. *arXiv preprint arXiv:2409.12191*, 2024. 2
- [42] Weiyun Wang, Zhangwei Gao, Lixin Gu, Hengjun Pu, Long Cui, Xingguang Wei, Zhaoyang Liu, Linglin Jing, Shenglong Ye, Jie Shao, et al. Internvl3. 5: Advancing open-source multimodal models in versatility, reasoning, and efficiency. *arXiv preprint arXiv:2508.18265*, 2025. 1, 2, 3, 7
- [43] Tianhao Wu, Chuanxia Zheng, Frank Guan, Andrea Vedaldi, and Tat-Jen Cham. Amodal3r: Amodal 3d reconstruction from occluded 2d images. *arXiv preprint arXiv:2503.13439*, 2025. 3
- [44] xAI. Grok-4, 2025. 2
- [45] Yan Xia, Ran Ding, Ziyuan Qin, Guanqi Zhan, Kaichen Zhou, Long Yang, Hao Dong, and Daniel Cremers. Targo: benchmarking target-driven object grasping under occlusions. *International Journal of Computer Vision (IJCV)*, 2025. 8
- [46] Katherine Xu, Lingzhi Zhang, and Jianbo Shi. Amodal completion via progressive mixed context diffusion. *Proceedings of the IEEE/CVF Conference on Computer Vision and Pattern Recognition (CVPR)*, 2024. 3
- [47] Qiyang Yu, Zheng Zhang, Ruofei Zhu, Yufeng Yuan, Xiaochen Zuo, Yu Yue, Weinan Dai, Tiantian Fan, Gaohong Liu, Lingjun Liu, Xin Liu, Haibin Lin, Zhiqi Lin, Bole Ma, Guangming Sheng, Yuxuan Tong, Chi Zhang, Mofan Zhang, Wang Zhang, Hang Zhu, Jinhua Zhu, Jiaye Chen, Jiangjie Chen, Chengyi Wang, Hongli Yu, Yuxuan Song, Xi-angpeng Wei, Hao Zhou, Jingjing Liu, Wei-Ying Ma, Ya-Qin Zhang, Lin Yan, Mu Qiao, Yonghui Wu, and Mingxuan Wang. Dapo: An open-source llm reinforcement learning system at scale, 2025. 3, 6
- [48] Guanqi Zhan, Chuanxia Zheng, Weidi Xie, and Andrew Zisserman. Amodal ground truth and completion in the wild. *Proceedings of the IEEE/CVF Conference on Computer Vision and Pattern Recognition (CVPR)*, 2024. 3
- [49] Guanqi Zhan, Yuanpei Liu, Kai Han, Weidi Xie, and Andrew Zisserman. Elip: Enhanced visual-language foundation models for image retrieval. *Proceedings of the IEEE International Conference on Content-Based Multimedia Indexing (CBMI)*, 2025. 5
- [50] Xiaohang Zhan, Xingang Pan, Bo Dai, Ziwei Liu, Dahua Lin, and Chen Change Loy. Self-supervised scene de-occlusion. In *Proceedings of the IEEE/CVF Conference on Computer Vision and Pattern Recognition (CVPR)*, pages 3784–3792, 2020. 3
- [51] Jinguo Zhu, Weiyun Wang, Zhe Chen, Zhaoyang Liu, Shenglong Ye, Lixin Gu, Hao Tian, Yuchen Duan, Weijie Su, Jie Shao, et al. Internvl3: Exploring advanced training and test-time recipes for open-source multimodal models. *arXiv preprint arXiv:2504.10479*, 2025. 2, 3
- [52] Yan Zhu, Yuandong Tian, Dimitris Metaxas, and Piotr Dollár. Semantic amodal segmentation. In *Proceedings of the IEEE Conference on Computer Vision and Pattern Recognition (CVPR)*, pages 1464–1472, 2017. 3, 4, 5, 6, 16
- [53] Yixing Zhu, Qing Zhang, Yitong Wang, Yongwei Nie, and Wei-Shi Zheng. Entityerasure: Erasing entity cleanly via amodal entity segmentation and completion. In *Proceedings of the Computer Vision and Pattern Recognition Conference*, pages 28274–28283, 2025. 3

# Appendix

## A. Implementation Details

In this section, we provide the detailed experimental settings referenced in Section 5.1 and Section 5.2 of the main paper. Specifically, we report the hyperparameters used for RL rollout and training in Table 5, the sizes of the RL training datasets for different models in Table 6, and the inference configurations in Table 7. We also present the prompt templates used for various models and tasks in Figure 7.

### A.1. Details of RL Training

Hyper-parameters	RL of	RL of
	QwenVL Model Series	InternVL Model Series
<b>Training Parameters</b>		
epochs	5	5
batch size	256	256
clip_ratio $\epsilon$	0.2	0.2
reward weight $\alpha$	0.5	0.5
KL weight $\beta$	0.005	0.0
Entropy weight $\gamma$	0.0	0.01
LR	3e-6	3e-6
LR warmup steps	30	30
LR scheduler name	cosine	cosine
max_response_length	1024	1024
n_samples	16	16
per device train batch size	32	32
dtype	float32	float32
<b>Rollout Parameters</b>		
temperature	0.7	0.7
top_p	0.9	0.7
top_k	50	-1
context size	32768	32768
per device rollout batch size	32	32
dtype	float16	float16

Table 5. **Hyperparameters for RL Training and Rollout.** In the VeRL configuration, setting `top_k = -1` disables top- $k$  filtering and is equivalent to using the full vocabulary.

We report the hyperparameters for RL training and rollout in Table 5.

Model	#Samples
InternVL-3-1B	100,600
InternVL-3-2B	63,887
InternVL-3-8B	37,574
Qwen3-VL-2B-Thinking	111,093
Qwen3-VL-4B-Thinking	79,319
Qwen3-VL-8B-Thinking	83,989

Table 6. **RL training dataset sizes.** All datasets are constructed using the learnability-based selection method detailed in Section 4.2. Dataset sizes vary across models due to differences in learnability distributions.

The RL training dataset sizes are presented in Table 6. The dataset is constructed strictly following the learnability-based procedure described in Section 4.2.

## A.2. Details of Model Inference

Parameters	Inference
temperature	0.0
top_p	1.0
top_k	20
max length	4096
repetition penalty	1.0

Table 7. **Parameters of Model Inference.**

We report the inference parameters in Table 7. These settings are used consistently throughout the RL training data construction process described in Section 4.2, as well as for all evaluation procedures in Section 5. To ensure fairness, we apply the same inference configuration to all models, which may lead to minor deviations from the official reported results for certain models.

```
# QwenVL Vanilla Grounding
Locate {sent}, output its bbox coordinates using JSON format.
# QwenVL Amodal Grounding
Locate {sent} amodally, output its amodal bbox coordinates using JSON format
# InternVL Vanilla Grounding
Please provide the bounding box coordinate of the region this sentence describes: <ref>{sent}</ref>
# InternVL Amodal Grounding
Please provide the amodal bounding box coordinate of the region this sentence describes: <ref>{sent}</ref>
```

Figure 7. **Prompt for training and inference of models from two different families.**

In Figure 7, we present the prompts used for two models across the two tasks. All vanilla grounding prompts are directly from the reference examples provided in the official GitHub repository, while the amodal grounding prompts are derived by modifying the corresponding vanilla grounding prompts.

## B. Details of Grounding Data Curation

As mentioned in Section 4 of the main paper, in this section we provide details of the data curation for vanilla and amodal training data.

You are looking at an image with a visual grounding task. The image shows a green bounding box indicating the Ground Truth (GT) target object.

Question: "{question}"

Ground Truth bbox (normalized 0-999 coordinates): {gt\_bbox}, which is highlighted as a green bbox on the input image.

Please analyze this visual grounding case and **explain how to correctly output the Ground Truth bbox according to the text description** of the Question, especially when there are **multiple similar objects**.

Please provide a **clear and concise analysis focusing on the visual reasoning process** in 1-2 sentences. Don't say 'green bbox' in your answer. The answer you give is going to be used to train a small model, so you should pretend not to know the GT bbox before hand. Just answer the question with reasoning.

Figure 8. Prompt for vanilla grounding reasoning dataset generation.

**Details of Vanilla Grounding Data Curation.** As in Figure 8, we provide the prompt to GPT-4 for the generation of the reasoning data of vanilla grounding training.

**Details of Amodal Grounding Data Curation.** Different from vanilla grounding, there is no off-the-shelf data for training that provides both the text prompt and the corresponding amodal bounding box. Existing amodal datasets, such as COCO-Amodal [52] and TAO-Amodal [16], provide ground truth annotations of amodal bounding box  $B_i$  of occluded objects, but there is only a short category name  $C_i$  for each object and no text prompt that can uniquely specify the target object in the image. To bridge the gap, we ask a proprietary VLM, *e.g.*, GPT-4 [17], to generate a more detailed description  $T_i$  of the target object in the RefCOCO prompt style. Figure 9 displays the prompt to GPT-4 for text prompt generation. The generated text prompt can be noisy and we further conduct a verification step: we feed the generated text prompt  $T_i$ , object bounding box  $B_i$  and the image  $I_i$  into the proprietary VLM (*i.e.*, GPT-4), and ask the VLM to verify whether the generated text prompt can accurately and uniquely specify the target object in the image. This verification step filtered out about 50% of the generated samples. The GPT-4 prompt for the verification step is in Figure 10.

Once we obtain the text prompt  $T_i$  associated with amodal bounding box  $B_i$ , we generate the reasoning process  $R_i$  via the same pipeline as introduced for vanilla grounding. The only difference is, in addition to how to locate the target object, the reasoning should also involve 1) what object(s) are causing the occlusion; 2) what this object's complete unoccluded shape looks like; 3) therefore, to recover the complete object, in which direction(s) and how much should be extended from the visible part. The detailed prompt to generate the amodal reasoning process is in Figure 11.

You are helping with a visual grounding task. I have added a TEMPORARY green box to mark the location of a {object\_category} in this image.

CRITICAL INSTRUCTIONS:

- The green box/rectangle/border is ARTIFICIAL and was added by me
- The green color is NOT part of the actual {object\_category}
- Ignore the green box completely when describing the object
- DO NOT mention: "green box", "green border", "green outline", "green frame", "marked in green", or any reference to green artificial markers
- If the object itself is naturally green (like grass or leaves), that's fine to mention
- But DO NOT describe anything green that is part of my annotation

Your task: Provide a concise description that uniquely identifies THIS specific {object\_category} in the image.

Requirements:

1. Length: 5-15 words
2. Must **uniquely identify this object** (not confusable with other objects)
3. Use spatial relationships for multiple similar objects:
  - Ordinal: "the second/third/fourth xxx from left/right/top/bottom"
  - Position: "the leftmost/rightmost/topmost/bottommost xxx"
  - Location: "xxx in the top-left/center/bottom-right"
  - Relative: "xxx behind/next to/above/below the yyy"
4. Describe natural features: position, appearance, color (of the actual object, not the annotation), state
5. Use lowercase, **natural referring expression style**

Good examples:

- "the man in yellow coat"
- "the second teddy bear from left"
- "the rightmost hot dog in the container"
- "woman in coveralls at the back"
- "the white computer screen that is on"
- "top sandwich in the left container"

Bad examples (DO NOT do this):

- "the object marked with green box" ❌
- "the item with green border" ❌
- "the magnet outlined in green" ❌

Now describe this {object\_category} (ignore my green annotation)

Figure 9. Prompt for amodal grounding prompt generation.

Look at this image. There is a region marked with a RED box and labeled "TARGET".

Your task: Determine if the following description **UNIQUELY and ACCURATELY identifies the TARGET region**:

Description: "{description}"

Please carefully check:

1. Does the description match the object/region inside the TARGET box?
2. Is the description specific enough that it couldn't refer to any other object in the image?
3. Would someone reading this description be able to locate exactly this TARGET region and no other?

Respond with **ONLY ONE WORD**:

- "YES" if the description uniquely and accurately identifies the TARGET region
- "NO" if the description is ambiguous, incorrect, or could refer to multiple objects

Your response (YES or NO):

Figure 10. **Prompt for amodal grounding prompt verification.**

You are analyzing an amodal object detection task. The image shows two bounding boxes:

- RED box: Modal bounding box (visible part of the object only)
- GREEN box: Amodal bounding box (complete object including parts occluded by OTHER OBJECTS)

Object description: "{question}"  
Image dimensions: {width} x {height} pixels

The complete object should be expanded in the following direction(s): {guidance\_str}

IMPORTANT: The red and green bounding boxes are added by us for your reference. They are NOT part of the original image. In your response, DO NOT mention the colored boxes, bounding boxes, or technical terms like "modal", "amodal", "bbox", or "IoU". Describe only what you see in the actual image.

Your task:

**\*\*IMPORTANT: Your ENTIRE response must be NO MORE THAN 5 SENTENCES TOTAL.\*\***

Provide a brief analysis:

1. How to **locate this object**
2. What object(s) are **causing the occlusion**
3. What does this object's **complete unoccluded shape** look like?
4. Therefore, to recover the complete object, explain in **which direction(s)** ({directions\_str}) and **how much** (using terms: "slightly", "a bit", "moderately", "considerably", or "significantly") should be extended from the visible part

Be extremely concise. Maximum 5 sentences. DO NOT mention: specific pixel values, image boundaries, red/green boxes, bounding boxes, modal/amodal, bbox, or IoU. DO NOT add concluding sentences about reasoning, spatial understanding, or detection accuracy.

Figure 11. Prompt for amodal grounding reasoning dataset generation.

## C. Qualitative Results

As mentioned in Section 5.6 of the main paper, in this section we show more qualitative results of our method on the Qwen family (Figure 6) and InternVL family (Figure 12).

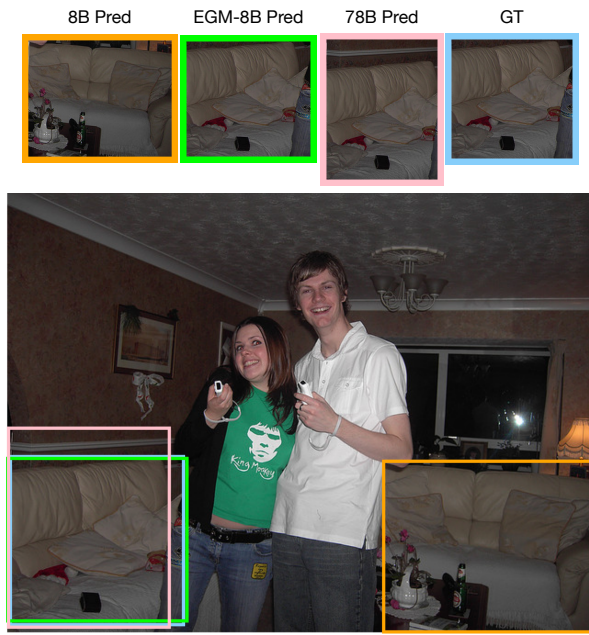
Figure 6 shows the qualitative comparison of Qwen3-VL-8B, Qwen3-VL-235B, and our EGM-Qwen3-VL-8B for vanilla grounding and amodal grounding. Besides the analysis in the main paper Section 5.6, here we also detail the reasoning process of the Qwen3-VL-235B model.

The Qwen3-VL-235B model also has its reasoning for the thinking model, but the reasoning process is much less efficient than ours. For the top left example of Figure 6, the entire reasoning of the Qwen3 model is “Got it, let’s see. The problem is to find the girl third from the right in the front row. First, I need to identify the front row. The front row is the group of girls standing in the front, not the ones behind. Let’s count from the right. The rightmost person is the one standing furthest to the right. Let’s list them: first, second, third. Let’s list the front row girls: Looking at the image, the front row (the main group) has several girls. Let’s count from the right: 1. Rightmost: girl with white tank top, green skirt, holding racket. 2. Second from right: girl with white cap, green skirt, holding racket. 3. Third from right: the one in white tank top, green skirt, between the cap girl and the next. Wait, let’s check. Wait, the front row’s count differs. Let’s see: front row left to right in front row: 1. Girl in green shirt and white skirt (coach maybe?). 2. Then the girls in white tops and green skirts. Let’s count the players in the front row (excluding the coach). Let’s see: from right to left: 1. Rightmost player: girl with white top, green skirt, holding racket. 2. Second: girl with white cap, green skirt, holding racket. 3. Third from right: the girl in white top, green skirt, between the cap girl and the next. Let’s check the image. Looking at the image, let’s count from the right: - First (rightmost): [838, 129, 993, 999] - Second: [742, 299, 922, 999] - Third from right: [635, 711, 771, 999]. Yes, that’s the ‘third from the right’. Let’s confirm. The third from the right in the front row (players) is the girl with the white top, green skirt, and she’s standing next to the girl with the white cap. So the bounding box for that girl is [635, 711, 771, 999].” It can be observed that the reasoning process contains lots of redundant words, and therefore is much less efficient than our EGM reasoning, which concisely focuses on the key feature that distinguishes the target object, as displayed on the bottom of the example in Figure 6 top left.

Figure 12 shows the qualitative comparison of InternVL-3-8B, InternVL-3-78B, and our EGM-InternVL-3-8B for vanilla grounding and amodal grounding.

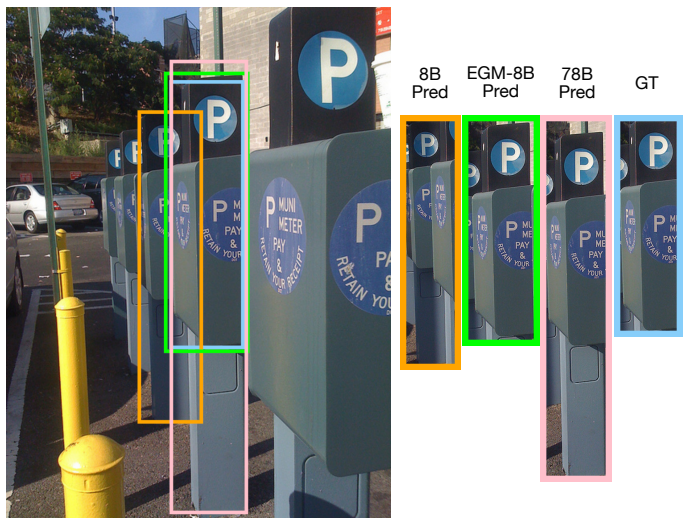
The top left, top right and bottom left samples are vanilla grounding on RefCOCO benchmark. For the *top left* example, the text prompt is ‘sofa against the wall’, and the InternVL-3-8B model mis-locates to another sofa. Our EGM-InternVL-3-8B correctly reasons the key feature ‘directly adjacent to the wall’ and generates a correct prediction. For the *top right* example, the text prompt is ‘sandwich between egg sandwiches’, and the InternVL-3-8B model confuses it with another sandwich. Our EGM-InternVL-3-8B, however, correctly reasons about the key feature ‘visually positioned between two others that appear to have egg filling’ and outputs the correct grounding box. For the *bottom left* example, the text prompt is ‘second P from the closest to us’, and the InternVL-3-8B model fails to understand ‘second’ and mis-predicts the ‘third’ P. Our EGM-InternVL-3-8B correctly predicts the correct ‘second P’, with a reasoning that it should be the ‘second one from the frontmost position’. For the vanilla grounding cases, generally InternVL-3-78B performs better than InternVL-3-8B, as can be observed in the examples.

The *bottom right* example is amodal grounding on the COCO-Amodal benchmark. It can be observed that InternVL-3-8B and InternVL-3-78B fail to predict the amodal grounding box of ‘the vertical metal pole behind the seated man’, while our EGM-InternVL-3-8B prediction is close to the ground truth, with reasoning process about locating the occluded metal pole, analyzing it is occluded by the seated man and should extend downward to recover the full unoccluded shape. This reasoning helps EGM-InternVL-3-8B to precisely locate the amodal bounding box covering both the visible and occluded parts of the metal pole.



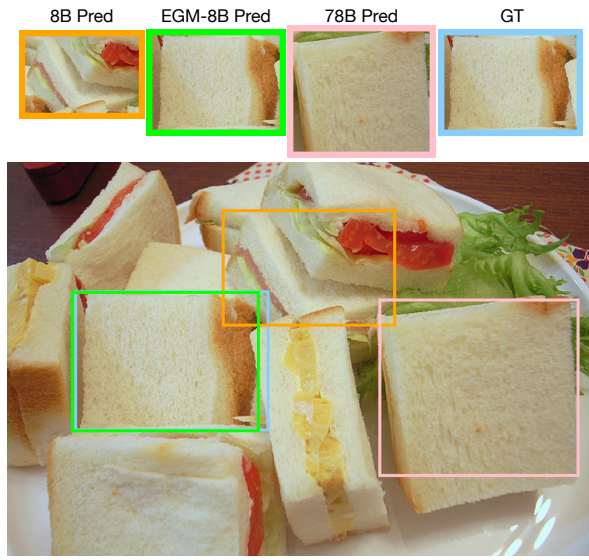
**Text Prompt:** sofa against the wall

**EGM Reasoning:** To correctly identify the bounding box for "sofa against the wall", focus on the object that is **directly adjacent to the wall** and matches the description of a sofa. In this image, the sofa is positioned along the left side, directly next to the wall, distinguishing it from other similar objects in the scene.



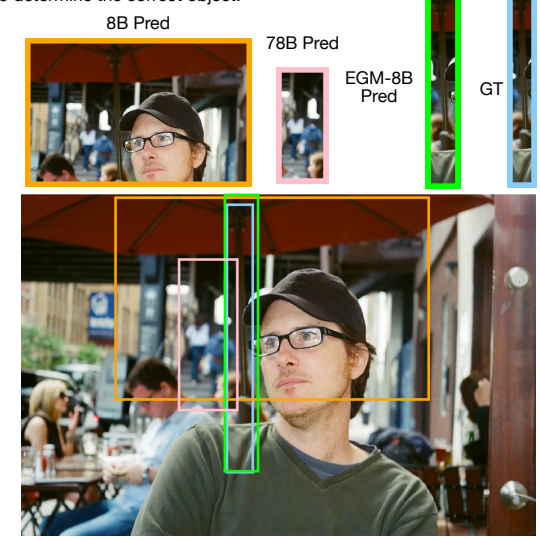
**Text Prompt:** second p from the closest to us

**EGM Reasoning:** To identify the correct object based on the description "second p from the closest to us", locate the sequence of similar objects (parking meters) and **select the second one from the frontmost position**. The bounding box should encompass this second object in the sequence.



**Text Prompt:** sandwich between egg sandwiches

**EGM Reasoning:** To identify the "sandwich between egg sandwiches", locate the sandwich that is **visually positioned between two others that appear to have egg filling**. Focus on the spatial arrangement and the distinct appearance of the egg filling to determine the correct object.



**Text Prompt:** the vertical metal pole behind the seated man

**EGM Reasoning:** The vertical metal pole is positioned centrally in the image, extending from the ground upward and partially hidden by the seated man. The **seated man is causing the occlusion**, blocking the lower and right portions of the pole. The complete shape of the pole is a long, straight cylinder that continues downward and to the right, likely reaching the ground. To recover the full object, **extend moderately to the right and considerably downward** from the visible part. The pole's base and lower segment are hidden behind the man's torso and arm.

Figure 12. **Qualitative comparison** of InternVL-3-8B, InternVL-3-78B, and our EGM-InternVL-3-8B for vanilla grounding and amodal grounding. Vanilla grounding: top left, top right and bottom left; Amodal grounding: bottom right.

## D. GPT Prompt for Failure Case Analysis

As mentioned in Section 3 of the main paper, Figure 13 shows the GPT prompt we used to analyze the failure reason of small VLMs. It can be seen that the failure reasons are categorized into 5 categories: ‘COMPLEX\_PROMPT’, ‘AMBIGUOUS\_IMAGE’, ‘SMALL\_OBJECT’, ‘GT\_ERROR’ and ‘Other’.

Analyze this visual grounding failure case. The image shows:

- Green box: Ground Truth (correct answer)
- Red box: Model's prediction

Task details: Question: "{question}" Model's prediction (0-999 coordinates): {pred\_bbox\_norm} Ground Truth (0-999 coordinates): {gt\_bbox\_norm} IoU: {iou:.3f}

Please analyze this failure and categorize it into ONE of the following categories:

- 1. COMPLEX\_PROMPT:** The text prompt contains complex linguistic elements that make it difficult:
  - Spatial relationships (e.g., "left of", "below", "between", "in front of")
  - Ordinal numbers (e.g., "first", "second", "third")
  - Relative descriptions (e.g., "closest to", "farthest from")
  - Compositional reasoning (e.g., "the red car next to the blue building")AND the image contains multiple similar objects that could be confused.
- 2. AMBIGUOUS\_IMAGE:** The image itself is ambiguous or contains very similar objects, but the prompt is relatively simple.
- 3. SMALL\_OBJECT:** The target object is very small or hard to see in the image.
- 4. GT\_ERROR:** The ground truth annotation appears to be incorrect or questionable based on the question and image.
- 5. OTHER:** Other types of failures not covered above.

Provide your analysis in this EXACT format:

```
<category> [One of: COMPLEX_PROMPT, AMBIGUOUS_IMAGE, SMALL_OBJECT, GT_ERROR, OTHER] </category>  
<reasoning> [2-3 sentences explaining why you chose this category. Be specific about what makes the prompt complex (if COMPLEX_PROMPT), what makes the GT questionable (if GT_ERROR), etc.] </reasoning>  
<confidence> [high/medium/low] </confidence>
```

Focus on the actual visual content, not the box colors.

Figure 13. The GPT prompt to analyze failure reasons of small VLMs.